

## INVESTIGATIONS OF STRUCTURAL VIBRATIONAL AND OPTICAL PROPERTIES OF MACKINAWITE NANOSTRUCTURED FeS FILM

TULAY HURMA\* , SABIHA AKSAY

Department of Physics, Anadolu University, TR-26470, Eskisehir, Turkey

*Iron sulphide nanocrystalline (FeS NCs) may have significant potential for applications in many areas. Ultrasonic spray pyrolysis (USP) method is used to deposit mackinawite FeS NCs film on glass substrate at 335 °C in this study. The film was characterized by vibrational (FTIR and Raman) spectroscopy, X-ray diffraction (XRD), scanning electron microscopy (SEM) and UV-vis spectra. The observed diffraction peaks at  $2\theta$  angles 28.12° and 50.45° correspond to the lattice planes (103) and (112) respectively. The crystallite size was calculated to be around 10 nm by using the Scherrer equation with the peak corresponding to the (112) plane. Raman spectrum revealed four peaks placed in the region of 200-750  $\text{cm}^{-1}$  due to mackinawite FeS phase. FTIR spectrum revealed two peaks at 649  $\text{cm}^{-1}$  and 827  $\text{cm}^{-1}$  that are attributed to stretching frequency of FeS. Optical band gap of the FeS film was determined to be 2.52 eV. Refractive index, extinction coefficient and optical conductivity of this film were determined using transmittance and reflectance spectra.*

**Keywords:** FeS film; Mackinawite; XRD; Raman; FTIR; Optical properties

### 1. Introduction

The studies done on nanosize materials have recently been showing great development in becoming an important exclusive field. They are divided into various classes as nanocrystals, nanoparticles, nanotubes, nanowires or nanostructure thin films. The main reason of focusing on this subject is that materials show extraordinary characteristics and functionalities different to their bulk forms in specific size range [1, 2]. The nanocrystalline materials in the form of a thin film allow to dramatically increase the basic characteristic properties such as optical, mechanical, electrical etc. for materials and tools produced by these materials. Due to increasing number of particles forming materials, a gradual transition from solid form to molecular form is observed. Furthermore, as the crystal size of a thin film affects the band form of a material, adequate small size of particles forming materials causes the load bearers at the quantum limit and the separation of band structures into intermittent energy levels [3]. Currently, the rapid change of thin film materials and their production creates new opportunities for developing new processes, materials and technologies. The synthesis of transition metal *chalcogenides* in the form of thin film, particularly metal sulfides have been of great

interest due to their possible use in modern optoelectronic devices, biological applications and solar energy. Among these materials, iron chalcogenides are of great interest because of their important photovoltaic, optoelectronic semiconducting, and structural properties [4, 5]. Recently, FeS nanomaterials, acting as a novel electrode material, possesses excellent catalytic and electrochemical properties and has drawn considerable research interests in many nonconventional applications, such as sensors, alkaline secondary batteries, lithium ion batteries, superconductors and solar energy materials [6-8]. Moreover, its abundance and non-toxicity are also reasons for the enormous interest in FeS. Most of the materials reported so far are either toxic or non-abundant such as cadmium, lead, indium and selenium, which means that these materials can not contribute significantly to a future sustainable energy needs [4]. Fe-S system exists in several modifications, which include: pyrite (cubic-  $\text{FeS}_2$ ), mackinawite (tetragonal  $\text{Fe}_{1+x}\text{S}$ ), marcasite (calcium chloride structure  $-\text{FeS}_2$ ), pyrrhotite ( $\text{Fe}_{1-x}\text{S}$ ,  $\text{Fe}_7\text{S}_8$ ), greigite (cubic spinel- $\text{Fe}_3\text{S}_4$ ), smythite (hexagonal- $\text{Fe}_3\text{S}_4$ ) and troilite (FeS) [9-11]. Small stoichiometry variations in the FeS structure cause large changes in physical, chemical and optical properties. FeS stoichiometric ratio is also closely related to the preparation method and reaction temperature [12]. In this study, nanostructured

\* Autor corespondent/Corresponding author,  
E-mail: [tulayhurma@gmail.com](mailto:tulayhurma@gmail.com)

mackinawite FeS film was obtained by spray pyrolysis method. The spraying method is spraying the aqueous solutions prepared for the films to be obtained by atomizing them on the hot substrate with the help of air or nitrogen gas. The spray pyrolysis method is one of the easiest and cheapest methods of obtaining thin films. Film quality varies with experimental parameters such as base temperature, spray rate and film thickness. If the two structures are pretty close with almost identical lattice parameters then it may be difficult to identify which of the two phases is the sample. Raman spectroscopy is an approved method to study qualitative and quantitative contribution of the phases [13-15], as well as possible secondary phases [16]. For this reasons, X-ray diffraction, Raman and FTIR spectroscopy were used to determine the crystal structure and identify the organic species present in the FeS film obtained by spray pyrolysis method at 335 ° C glass substrate temperature. Other experimental techniques, such as, UV-vis spectra, scanning electron microscopy have been used in order to achieve accurate knowledge of the optical properties and surface morphology of the mackinawite FeS NCs film.

## 2. Experimental details

50 ml (0.05 M) FeCl<sub>6</sub>H<sub>2</sub>O and 50 ml (0.05 M) SC (NH<sub>2</sub>)<sub>2</sub> were taken as a precursor solution to obtain FeS NCs film. Substrate temperature was kept constant at 335±5 °C using Fluke 62 max infrared thermometer. Experimental details for deposition can be found in our previous work [17]. For XRD measurements X-ray powder diffractometer (BRUKER D8 Advance) was used. **The Raman spectrum of the film was recorded in 0-1750 cm<sup>-1</sup> range on a Bruker Senterra Dispersive Raman instrument using laser excitation with the wavelength of 632.8 nm. FT-IR spectra were recorded on a Perkin Elmer 2000 FT-IR spectrometer in the wavenumbers of 500-4000 cm<sup>-1</sup> at room temperature by using ATR (4 cm<sup>-1</sup> resolution).** For the optical reflectance and transmittance measurements of FeS film, we used a double beam Shimadzu 2450 UV-spectrophotometer with an integrating sphere attachment in 200-900 nm wavelength range. Surface morphology of the film was studied using ZEISS Ultra plus model field emission scanning electron microscopy (FESEM) at 10 kV.

## 3. Results and discussion

### 3.1. XRD-FESEM studies of the FeS NCs film

XRD is an analytic technique which allows us to get information on various crystal forms or phases in structures of solid and powder materials. The diffraction peaks of FeS NCs film are illustrated in Figure 1.

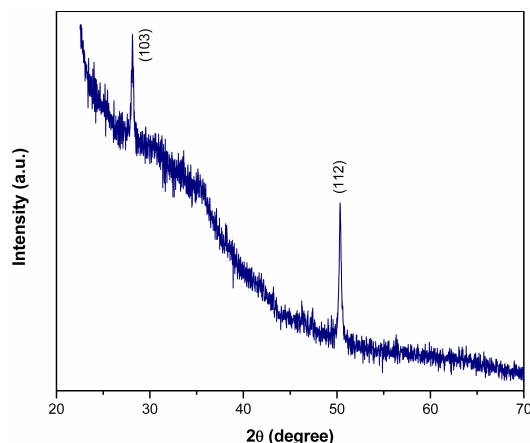


Fig. 1 - XRD pattern of the mackinawite FeS NCs film.

As it is seen in these figure, the observed diffraction peaks at 2θ angles 28,12° and 50,45° correspond to the lattice planes (103) and (112) respectively [18, 19]. According to the XRD spectrum, it can be said that FeS film produced on glass substrate is preferentially in mackinawite FeS (112) crystal form. Crystallite size can be smaller than grain size or particle size. Crystallites are coherent diffraction zones in X-ray diffraction. The results obtained from SEM images are usually related to grain size. The crystallite size (D) of the films for the peak with highest intensity can also be estimated by using Scherrer's formula [20],

$$D = \frac{0.9\lambda}{\beta \cos \theta} \quad (1)$$

where λ is the X-ray wavelength used, β is the angular line width of maximum intensity, and θ is Bragg's diffraction angle. The crystallite size of the FeS was calculated to be around 10 nm by using the Scherrer equation [20] with the peak corresponding to the (112) plane. The average grain size and surface morphology of the FeS NCs film were determined by SEM. The SEM images are shown in Fig.2 (a) and (b) with magnifications of 20,000× and 100,000×.respectively. As seen in Fig. 2, glass surface is fully covered with irregular distributed spherical grains. From the SEM images, it was observed FeS film well adhered to the glass substrates. The average particle size was around 12 nm, similar to the result obtained from XRD measurement.

### 3.2. Raman and FT-IR analysis

Raman spectroscopy, a vibrational spectroscopic method based on inelastic scattering of light, is an approved method for characterization of FeS phases [21-24] as well as possible secondary phases [25]. Figure 3 shows the Raman spectrum of FeS NCs film in the frequency region of 50-1750 cm<sup>-1</sup>. Raman spectrum revealed four peaks that are situated at 208 cm<sup>-1</sup>, 271 cm<sup>-1</sup> 382 cm<sup>-1</sup> 581 cm<sup>-1</sup> of the spectrum due to mackinawite FeS phase [21].

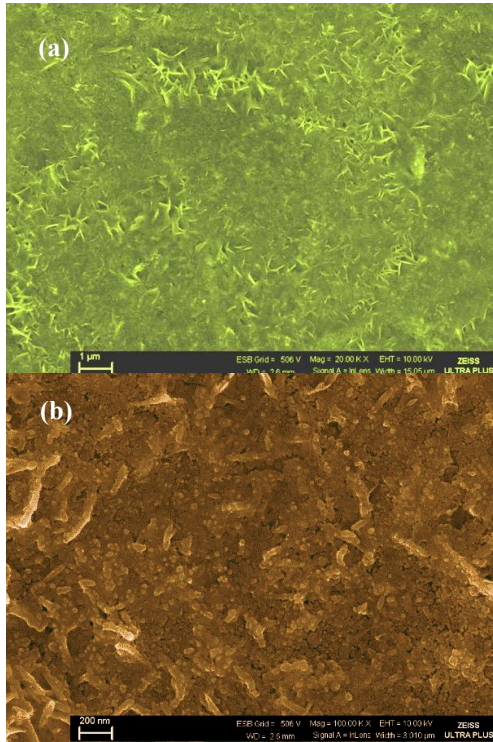


Fig. 2 - SEM image of the mackinawite FeS NCs film.

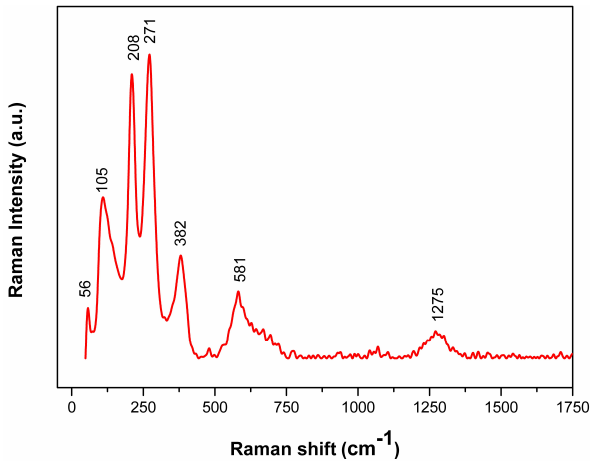


Fig. 3 - Raman spectrum of the mackinawite FeS NCs film.

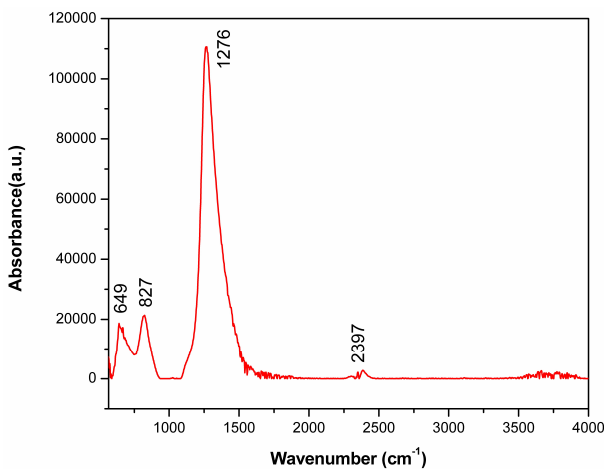


Fig. 4. FTIR spectrum of the mackinawite FeS NCs film.

Less intense broad hump-like feature around 1275  $\text{cm}^{-1}$ , in the high frequency region due to  $\text{Fe}_2\text{O}_3$  phase [16, 21] is noticed. XRD measurement did not detect the existence of the  $\text{Fe}_2\text{O}_3$  phase. It is technically challenging to detect or identify any phase via XRD if it has a very small volume percentage of poorly formed crystallites. In contrast to X-ray diffraction, Raman spectroscopy provides more information about the defect phases because it is sensitive to local symmetry. Low energy Raman mode lattice vibrations around 56  $\text{cm}^{-1}$  and around 105  $\text{cm}^{-1}$  were, however, also observed. Particles of nanometric size show low wavenumber vibrational modes that can be observed by Raman spectroscopy [26]. More recent quantitative investigations into the chemistry of semiconductor film have used FTIR spectroscopy together with the XRD and Raman spectroscopy. The characteristic peaks exhibited by FTIR absorption spectrum of FeS film at room temperature in the wavenumber range of 500 to 4000  $\text{cm}^{-1}$  are shown in Fig. 4. There are two peaks at 649  $\text{cm}^{-1}$  and 827  $\text{cm}^{-1}$  that may be attributed to stretching frequency of FeS bond. A strong band at 1276  $\text{cm}^{-1}$  due to the Fe-O stretching bands, is also noted. The spectrum indicated the absorption at 2397  $\text{cm}^{-1}$  (weak), which is assigned to  $\text{CO}_2$  molecule in air and it is not related to the film.

**3.3. Optical properties**

Optical properties of FeS NCs were investigated with UV-vis spectroscopy. The optical transmittance and reflectance spectra (inset the plot of  $(\alpha h\nu)^2$  vs  $h\nu$ ) for FeS NCs film in the wavelength range of 200–900 nm are shown in Figure 5.

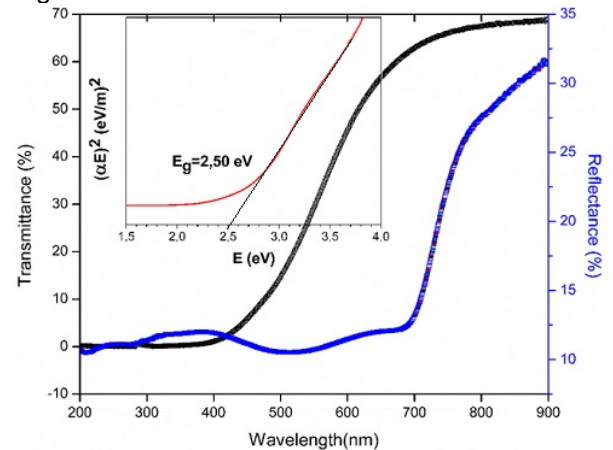


Fig. 5 - The optical transmittance and reflectance spectra (inset the plot of  $(\alpha h\nu)^2$  vs  $h\nu$ ) for FeS NCs film.

As seen in these curves, the transmittance value starts to increase at 400 nm and reaches its maximum value at 900 nm. It is seen that the reflectance value of the film is minimum up to 700 nm and there is an increase within 700-900 nm range by increasing wavelength of the light. It has

been determined that in the visible region the film has almost no reflectance and the maximum transmittance value is about 70%. The optical band gap is evaluated according to the well-known Tauc's relation [27]:

$$\alpha E = A(E - E_g)^m \quad (2)$$

where  $A$  is a constant,  $\alpha$  is the absorption coefficient,  $E$  is the photon energy and  $E_g$  is the optical band gap. The exponent  $m$  depends on the nature of the transition,  $m=1/2, 2, 3/2$  or  $3$  for allowed direct, allowed indirect, forbidden direct or forbidden indirect transitions, respectively. Inset of Figure 5 shows the plots of  $(\alpha E)^2$  vs  $E$  for the film. The studies on the band structure of FeS using Eq. (2) [27] resulted in the direct allowed transition associated band gap for the tetragonal mackinawite FeS film. The band gap can be obtained by extrapolating the linear portion of the plot  $(\alpha E)^2$  vs  $E$  to  $\alpha = 0$ . Optical band gap of the tetragonal mackinawite FeS film was found to be 2.50 eV with a direct optical transition. The higher band gap energy compared to that of the bulk FeS material is due to the smaller particles size (~10 nm) of the film. The previously reported forbidden energy range for bulk FeS is 0.04 eV [6] The increase of the band gap has been attributed to the defects and secondary phases. Secondary Fe-O phases were already detected by Raman and FTIR spectroscopy. Besides that is well known that when the size of particles decrease into the nanoscale range, the band gap will increase due to quantum confinement effects, which means that smaller size leads to a larger band gap energy [28, 29]. In the bulk matter, the bands are actually a combination of multiple atoms and neighboring energy levels of the molecule. When the particle size reaches the nano scale, where each particle is composed of a very small number of atoms or molecules, the number of overlaps of the orbitals or the energy level is reduced and the width of the bands is narrowed. This causes an increase in energy gap between the valance band and the conduction band [30]. The non-toxic FeS NCs film with expanded energy range obtained in this study, can be applied for solar energy harvesting. The refractive index of the film was calculated by the following equation [31]:

$$n = \left( \frac{1+R}{1-R} \right) - \sqrt{\frac{4R}{(1-R)^2} - k^2} \quad (3)$$

In this equation,  $k$ , extinction coefficient is expressed as  $k = \alpha\lambda/4\pi$  equation while  $R$  is the reflectance.

The refractive index and extinction coefficient values of the film are shown in Figures 6-7 respectively.

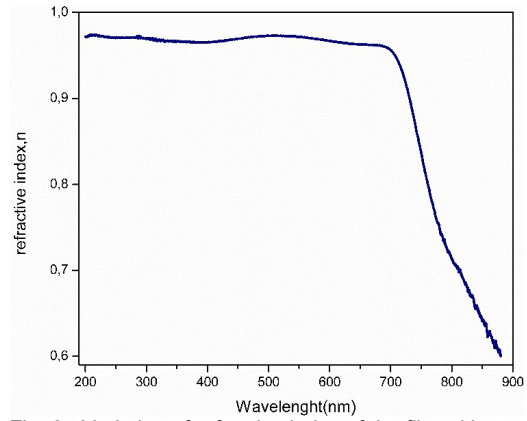


Fig. 6 - Variation of refractive index of the film with wavelength.

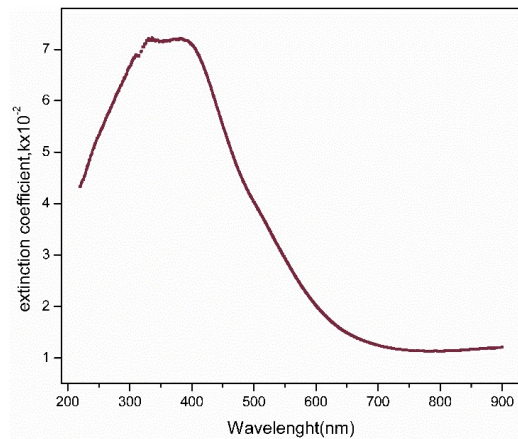


Fig. 7 - Variation of extinction coefficient of the film with wavelength.

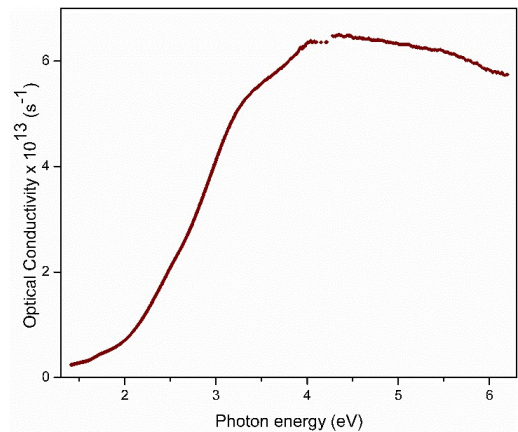


Fig. 8 - Variation of optical conductivity of the film with photon energy.

The refractive index value which was at fixed and maximum range of 200-700 nm was quickly decreased to the minimum value in 700-900 nm range. The extinction coefficient has the maximum value in the 300-400 nm range by increasing 200-300 nm range and reached its minimum value by decreasing 400-700 nm range. The decrease in extinction coefficient with increase in wavelength show that the fraction of light is lost due to scattering and consequently absorbance decreases [16]. Optical conductivity is a powerful tool to measure electronic states of materials. Photoconductivity is a special case of optical

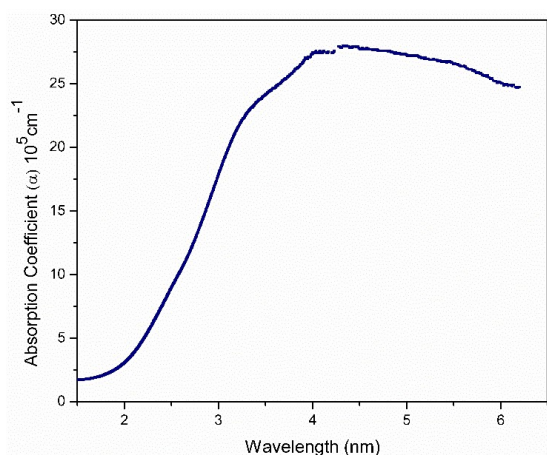


Fig.9 - Variation of absorption coefficient ( $\alpha$ ) of the film with wavelength.

conductivity. When the light falls on a semiconductor, it is transmitted to the electrons of the valence band, and the electrons of the valence band are excited to the emission band and the conductivity increases. The value of optical conductivity is related to the absorption coefficient ( $\alpha$ ), speed of light ( $c$ ) and the refractive index ( $n$ ) by the following expression [27].

$$\sigma = \frac{\alpha n c}{4\pi} \quad (4)$$

A plot of film's optical conductivity ( $\sigma$ ) as a function of photon energy ( $h\nu$ ) is given in Fig.8. Due to the fact that the absorption coefficient can be increased to this region, the optical conductivity is increased gradually by the photon energy up to 4.0 eV, and gradually decreased down to 6 eV. The optical conductivity directly depends on both the absorption coefficient (Fig.9) and the refractive index of the material and it is found to follow the same trend as that of the absorption coefficient and the refractive index with increasing wavelength.

#### 4. Conclusion

FeS NCs film prepared on glass substrate. XRD, Raman and FTIR techniques were used to analyze the chemical bonding and to characterize and identify the organic species present in the film. The XRD result suggests that the FeS NCs film has polycrystalline structure. The Raman spectrum revealed seven peaks of the film in the frequency region 50-2000  $\text{cm}^{-1}$ . The Raman bands inside the low-frequency region are assigned to acoustic modes related with the vibration of individual nanoparticles as a whole. Optical band gap of the film was found to be 2.50 eV with a direct optical transition. The refractive index, extinction coefficient and optical conductivity were calculated for the film.

#### Acknowledgement

We would like to thank Mrs. Özge Bağlayan for the Raman spectroscopy, Mrs. Seval Aksoy for SEM, Mrs. Büşra Avcı for UV-vis measurements and Mrs. Pınar Bilgiç Özden for XRD measurements.

#### REFERENCES

1. A.N. Goldstain, Handbook of Nanophase Materials, Marcel Dekker, New York, 1997.
2. C.N.R. Rao, A. Müller, A.K. Cheetham, The Chemistry of Nanomaterials, Wiley-VCH Verlag GmbH & Co. KgaA, Weinheim, 2005.
3. B. Pejova, I. Grozdanov, Structural and Optical Properties of Chemically Deposited Thin Films of Quantum-Sized Bismuth (III) Sulfide, Mater. Chem. and Phys., 2006, 99, 39.
4. M. Saeed Akhtar, A. Alenad, M. Azad Malik, Synthesis of mackinawite FeS thin films from acidic chemical baths, Mater. Sci. in Semiconductor Process., 2015, 32, 1.
5. A.K. Dutta, S. K. Maji, D. N. Srivastava, A. Mondal, P. Biswas, P. Paul, B. Adhikary, Synthesis of FeS and FeSe Nanoparticles from a Single Source Precursor: A Study of Their Photocatalytic Activity, Peroxidase-Like Behavior, and Electrochemical Sensing of  $\text{H}_2\text{O}_2$ , ACS Appl. Mater. Interfaces 2012, 4, 1919.
6. S. K. Majia, A. K. Duttaa, P. Biswasa, B. Karmakarb, A. Mondala, B. Adhikarya, Nanocrystalline FeS thin film used as an anode in photo-electrochemical solar cell and as hydrogen peroxide sensor, Sensors and Actuators B, 2012, 166, 726.
7. P.P. Chin, J. Ding, J.B. Yi, B.H. Liu, Synthesis of  $\text{FeS}_2$  and FeS nanoparticles by high-energy mechanical milling and mechanochemical processing, Journal of Alloys and Compounds, 2005, 390, 255.
8. E. Shangguan, F.Li, J. Li, Z. Chang, Q. Li, X.Z. Yuan, H. Wang, FeS/C composite as high-performance anode material for alkaline nickel-iron rechargeable batteries, Journal of Power Sources, 2015, 291, 29.
9. J.B. Goodenough, Structural chemistry of iron sulfides, Mater. Res. Bull., 1978, 13, 1305.
10. C.N.R. Rao, K.P.R. Pisharody, Transition metal sulfides, Prog. Solid State Chem., 1976, 10, 207.
11. A.R. Lennie, D.J. Vaughan, Spectroscopic studies of iron sulfide formation and phase relations at low temperatures, Mineral Spectroscopy, 1996, 5, 117.
12. S. Middya, A. Layek, A. Dey, P.P. Ray, Synthesis of Nanocrystalline  $\text{FeS}_2$  with increased band gap for solar energy harvesting, J. Mater. Sci. Technol., 2014, 30, 770.
13. T. Riedle, Raman Spectroscopy for the analysis of thin  $\text{CuInS}_2$  films, Doctoral thesis, Technical University of Berlin, 2002.
14. J. Alvarez-Carcia, A. Perez-Rodriguez, B. Barcones, A. Romando-Rodriguez, J. R. Morante, Polymorphism in  $\text{CuInS}_2$  epilayers: Origin of additional Raman modes, Appl. Phys. Lett., 2002, 80, 562.
15. J. Alvarez-Carcia, J. Marcos-Ruzafa, A. Perez-Rodriguez, A. Romano-Rodriguez, J. R. Morante, R. Scheer, MicroRaman scattering from polycrystalline  $\text{CuInS}_2$  films: structural analysis, Thin Solid Films, 2000, 361-362, 208.
16. P. Guha, D. Das, A. B. Maity, D. Ganguli, S. Chaudhuri, Synthesis of  $\text{CuInS}_2$  by chemical route: optical characterization, Sol. En. Mat. Sol. Cells, 2003, 80, 115.
17. T. Özer, S. Köse, Some physical properties of  $\text{Cd}_{1-x}\text{Sn}_x\text{S}$  films used as window layer in heterojunction solar cells, Int. J. Hydrogen Energy, 2009, 34, 5186.
18. S.G. Ibrahim, A.U. Ubale, Structural, electrical and optical properties of nanostructured  $\text{Cd}_{1-x}\text{Fe}_x\text{S}$  thin films deposited by chemical spray pyrolysis technique, Journal of Molecular Structure, 2014, 1076, 291.

19. M. S. Akhtar, A. Alenad, M. A. Mali, Synthesis of mackinawite FeS thin films from acidic chemical baths, Mater. Sci. in Semiconductor Process., 2015, **32**, 1.
20. B.D. Cullity, S.R. Stock, Elements of X-ray Diffraction, Prentice-Hall, New Jersey, 2001.
21. G. Genchev, A. Erbe, Raman spectroscopy of mackinawite FeS in anodic iron sulfide corrosion products, J. of the Electrochem. Society, 2016, **163**, 333.
22. J.A. Bourdoiseau, M. Jeannin, R. Sabot, C. Remazeilles, P. Refait, Characterisation of mackinawite by Raman spectroscopy: Effects of crystallisation, drying and oxidation, Corrosion Science, 2008, **50**, 3247.
23. R. Henriquez, C. Vasquez, N. Briones, E. Munoz, P. Leyton, E.A. Dalchiele, Single Phase FeS<sub>2</sub> (pyrite) Thin Films Prepared by Combined Electrodeposition and Hydrothermal Low Temperature Techniques, Int. J. Electrochem. Sci., 2016, **11**, 4966.
24. T. Ocampo-Macias, J. Lara-Romero, R. Huirache-Acuna, J.J. Alvarado-Flores, J. Lopez-Tinoco, F. Chinas-Castillo, S. Jimenez-Sandoval, F. Paraguay-Delgado, A. Reyes-Rojas, Synthesis of iron sulfide films through solid-gas reaction of iron with diethyl disulfide, Journal of Sulfur Chemistry, 2015, **36**, 385.
25. J. Lopez-Sanchez., A. Serrano, A. Del Campo, M. Abuin, O. Rodriguez de la Fuente, N. Carmona, Sol-gel synthesis and micro-Raman characterization of ε-Fe<sub>2</sub>O<sub>3</sub> micro- and nanoparticles, Chem. Mater., 2016, **28**, 511.
26. M. Ivanda, K. Furic, S. Music, M. Ristic, M. Gotic, D. Ristic, A. M. Tonejc, I. Djerdj, M. Mattarelli, M. Montagna, F. Rossi, M. Ferrari, A. Chiasera, Y. Jestin, G. C. Righini, W. Kiefer, R. R. Gonçalves, Low wavenumber Raman scattering of nanoparticles and nanocomposite materials, J. of Raman Spectroscopy, 2007, **38**, 647.
27. J. I. Pankove, Optical process in semiconductors, Prentice Hall Inc., New York, 1971.
28. M. L. Steigerwald, L. E. Brus, Semiconductor Crystallites a class of large molecules Accounts. Chem. Res., 1990, **23**, 183.
29. A. P. Alivisatos, Perspectives on the Physical Chemistry of Semiconductor Nanocrystals, J. Phys. Chem., 1996, **100**, 13226.
30. E. Roduner, Size matters: why nanomaterials are different, Chem. Soc. Rev., 2006, **35**, 583.
31. N.A. Subrahmanyam, A textbook of Optics, BRJ Laboratory, Delhi, 1977.

\*\*\*\*\*

**SCIENTIFIC EVENTS**

**24<sup>th</sup> World Nano Conference  
May 07-08, 2018 Rome, Italy**

**Theme: Invention and Innovation of New Concepts in the Field of Nanotechnology**

**Nano 2018** aims in proclaim knowledge and share new ideas amongst the professionals, industrialists and students from research areas of Nanotechnology, Materials Science, Chemistry and Physics to share their research experiences and indulge in interactive discussions and technical sessions at the event.

- Track 1: Nanoscience and Technology
- Track 2: Nano Medicine
- Track 3: Nano Electronics
- Track 4: Nano Materials Synthesis and Characterisation
- Track 5: Pharmaceutical Nanotechnology
- Track 6: Materials Science and Engineering Physics
- Track 7: Nanotechnology in Water Treatment
- Track 8: Advanced Nanomaterials
- Track 9: Carbon Nanotechnology
- Track 10: Nanotech for Energy and Environment
- Track 11: Nano Biotechnology
- Track 12: Nanobiomaterials
- Track 13: Nano Toxicology
- Track 14: Nanophotonics
- Track 15: Molecular Nanotechnology
- Track 16: Nanotechnology Safety
- Track 17: Nanotechnology in Tissue Engineering
- Track 18: Nanotechnology in Agriculture and Food Industry
- Track 19: Nano Fluidics
- Track 20: Nano Computational Modelling
- Track 21: Nano Composites
- Track 22: Nanoengineering
- Track 23: Graphene and its Applications

**Contact:** <https://nano.conferenceseries.com/>

\*\*\*\*\*